Fig. 5. Shows the FTIR spectrum of BPH

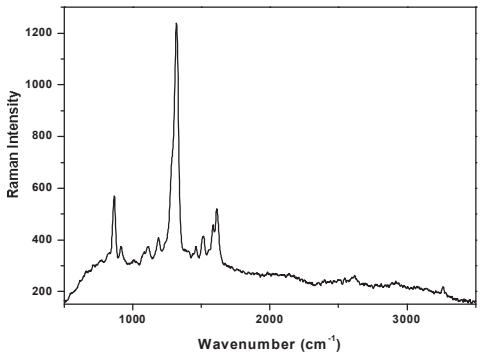

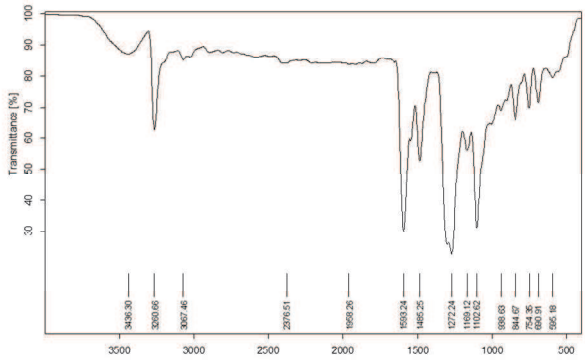

Fig.6. shows the FT Raman spectrum of BPH

Table 2. Observed IR and Raman bands of Benzaldehyde 4-nitro phenylhydrazone		
FTIR wavenumber (cm^{-1})	FT Raman wavenumber (cm^{-1})	Assignments
3436		υas(N-H)
3260		υas(N-H)
3067		υs(N-H)
2376		υ(C-H)
1958		υ(C-H)
	1612	δ(N-H)
1596		υ(C-C)
	1517	υas(NO2), υ(C-C)
1486	1457	ρ(N-H)
	1318	υs(NO2)
1271		δ(C-H)
1168	1184	υas(C-NO2)
1101	1114	φ ring
938	911	υ(C-C)
845	863	δ(C-H)
754		ω(NO2)
690		δring
595		τ(N-H)
νas- asymmetric stretching; νs-symmetric stretching; ρ - rocking; τ- torsion; ω- wagging; δ - deformation, φ -scissoring.		

The BPH crystallizes in the orthorhombic system, with Cc space group. As there are 29 atoms in the unit cell (Z=4), there are 348 branches to phonon dispersion curves. The representation of Γtotal of all vibrations can be decomposed according to the irreducible representation of the point group as Γ-total=173A′+ 172 A″ apart from three acoustic modes (Γacou = A′ + 2 A″) are included that correspond to the block transitions of the crystal. The formal classification of fundamental mode predicts 324 internal vibrations which can be distributed as (162A′+ 162 A″) and 24 external modes such as (6A′+6A″) translational, (6A′+6A″) vibrational modes. The results of factor group analysis are presented in Table 3.

Table 3 Factor group analysis-Summary

Factor group species Cs	Benzaldehyde 4-nitro phenylhydrazone C1 site		C C1 site	H C1 site	N C1 site	O C1 site	Optical modes	Acoustic modes	Activity	
Internal modes		External modes	Benzaldehyde 4 nitro phenylhydrazone C1 site						IR	Raman
A'	162	6T, 6R	78	66	18	12	174	01	Tx, Ty	αxx, αyy, αzz, αxy
A"	162	6T, 6R	78	66	18	12	174	02	Tz	αyz, αxz
Total modes	324	12T, 12R	156	132	36	24	348	03		

The hydrogen bonding networks seem to tailor the molecular dipoles of the ionic species in similar direction. The presence of the hydrogen bond besides the columbic interactions between the ionic species helps in building up stable structures and is also one of the favorable factors to have high melting point and to grow single crystals with relative ease. The importance of hyperconjugative interaction and electron density transfer from lone electron pairs of the Y atom to the X-H anti-bonding orbital in the X-H...Y system have been analyzed. The intermolecular N-H...O hydrogen bonding is formed due to the overlap between n(O) and σ*(N-H) which results in intermolecular charge transfer causing stabilization of H-bonded systems. Thus the broad bands with complicated structures in thi region 3400–3000 cm^{-1} corresponds to X-H stretching vibrations.

Generally N-H and O-H bands participate in hydrogen bonding, hence their stretching vibrations should be shifted to low wave number side and also they are asymmetric (νas). The symmetric stretching (νs) has no degeneracy. But the asymmetric stretching is doubly degenerate. This may be attributed to the lowering of symmetry in the crystal environment C1 than that of the free ion. Because of this lowering of symmetry, the degeneracy of the asymmetric stretching is raised and so one can observe two bands corresponding to νasNH vibrations. Hydrogen bond vibration is clearly seen in IR than in Raman spectra. In IR, the band corresponding to this mode is observed at 3436 and 3261 cm^{-1}. Further in the present investigation, this N-H stretching wave number is red shifted in IR, which indicates the weakening of the N-H bond resulting in proton transfer to the neighboring hydrogen. The nature and the strength of the intermolecular hydrogen bonding can be determined by knowing the changes of electron densities (ED) in the vicinity of N-H... hydrogen bonds, which lead to the increase in ED of N-H anti bonding orbital. This causes concomitant red shift in N-H stretching wave number(Alabugin et al 2003). An interesting feature of these vibrations is that, through these intermolecular interactions charge transfer can take place inside the crystal. This mechanism enhances the hyperpolarizability value which in turn responsible for the propensity of the crystal to be NLO active.

The bands observed in the region 2900–3100 cm^{-1} are assigned to the C-H stretching vibrations. In the present molecule the aromatic rings are asymmetrically disubstituted benzene derivatives. The bands corresponding at strong band 1596 cm^{-1} in IR and around very weak bands 1517 cm^{-1} in Raman are attributed to the Kekule C-C stretching mode. These

vibrations are expected to interact with C-H in plane bending hydrogen and its carbon moving oppositely but the substituents are nearly motionless (Spire et al 2000). The observed IR and Raman bands and their assignments are stacked in Table 2.

The region (1800-300 cm^{-1}) includes the stretching vibrations of amino groups and the bending vibrations of amino and methylene groups. The detailed vibrational assignments presented in Table 2 for various modes are self-explanatory. Since mixing of several groups is possible in this region it will be very difficult to distinguish the vibrations arising from various individual groups like C–C, deformation modes of N-H, C–H etc., and also functional group frequency correlation method will not work out for the accurate assignment of bands.

UV-VIS-NIR studies: When absorption is monitored from longer wavelength to shorter wavelength, the enhanced absorption is observed between 1500-2000 nm (Fig.7). The absorption in this region is due to overtones of some fundamental vibrations of nitro group. There is low absorption at the fundamental wavelength (1064 nm) of the Nd:YAG laser which contributes to its resistance to laser induced damage. Further there is very little absorption at the wavelength of 532 nm, which can improve the second harmonic throughput. Due to the weak inductive effects, the nitro group exerts a small shift in the absorption edge of BHP around 380 nm which recommends this as a better material for the fabrication of lased based spectral instruments and also good enough for the generation of higher harmonic light using IR lasers through NLO phenomena. Some absorption bands in the UV – visible region may be attributed to the colored centers within the forbidden gap of the material. It could pose some limits to the power handling capacity of this material.

Kurtz and Perry Powder Technique for SHG measurement:

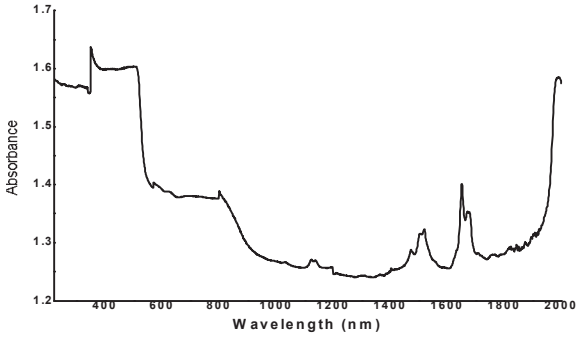

Fig.7.Shows the UV-Vis-NIR Spectrum of BPH

The Table 4 shows the comparison of SHG signal energy output for the title compound BPH with that of standard KDP and Urea. The high efficiency of BPH crystal is higher than KDP and Urea counterparts.

Table 4 Comparison of SHG signal energy output

Input power mJ/ pulse	KDP mV	Urea mV	BPH mV
1.9	9.0	----	162
3.0	---	100	213

Conclusion: A good optical quality crystal of BPH was obtained by slow evaporation solution growth method. The structural analysis of BPH was confirmed by powder x-ray diffraction analysis. The vibrational functional group of BPH was investigated and confirmed by FT-IR, FT-Raman and factor group analysis. In the transmittance spectra of BPH crystal has wide range transparency from visible to IR region. The SHG effect of BPH is higher than urea.

References:

1. D. A. Kleinman, "Nonlinear dielectric polarization in optical media," Phys. Rev. vol.126, pp.1977–1979, 1962.
2. L. Padmaja, T. Vijayakumar, I. Hubert Joe, C. P. Reghunadhan Nair and V. S. Jayakumar" Vibrational spectral studies and the non-linear optical properties of a novel NLO material L-prolinium Tartrate" J. Raman Spectrosc. vol. 37, pp.1427–1441, 2006
3. D.S.Chemla and J. Zyss, "Non-linear Optical Properties of Organic Molecules", Academic Press, Newyork, vol 1, 1987
4. A.A. Sukhorukov and Yu.S. Kivshar, "Nonlinear guided waves and spatial solitons in a periodic layered medium", J. Opt. Soc. Am. B, vol. 19, pp. 772-781, 2002.
5. G. Maroulis, "Static hyperpolarizability of the water dimer and the interaction hyperpolarizability of two water molecules", J. Chem. Phys. vol. 113, pp. 1813-1820, May2000
6. G. Maroulis, "Electric multipole moment, dipole and quadrupole(hyper)polarizability derivatives for HF ($X^1\Sigma^1$)" J. Mol. Struct. (Theochem). vol. 633, pp 177-197, 2003.
7. A.Schoonveld,.Wildeman, D.Fichou, P.A.Bobbert, B.J.Van Wees and T.M.Klapwijk, Nature, vol. 404, pp. 977, 2000.

***

Department of Physics,University College of Engineering Panruti
Panruti-607 106, Tamil Nadu, India,sril35@gmail.com
Departamento de Fisica,Universidade du Minho, Campus de Gualtar,
Portugal.